



NIR-Sensitized Activated Photoreaction between Cyanines and Oxime Esters: Free-Radical Photopolymerization

Yulian Pang, Shuheng Fan, Qunying Wang, Dennis Oprych, Alfred Feilen, Knut Reiner, Dietmar Keil, Yuriy L. Slominsky, Sergey Popov, Yingquan Zou,* and Bernd Strehmel*

Abstract: Cyanines comprising either a benzo[e]- or benzo-[c,d]indolium core facilitate initiation of radical photopolymerization combined with high power NIR-LED prototypes emitting at 805 nm, 860 nm, or 870 nm, while different oxime esters function as radical coinitiators. Radical photopolymerization followed an initiation mechanism based on the participation of excited states, requiring additional thermal energy to overcome an existing intrinsic activation barrier. Heat released by nonradiative deactivation of the sensitizer favored the system, even under conditions where a thermally activated photoinduced electron transfer controls the reaction protocol. The heat generated internally by the NIR sensitizer promotes generation of the initiating reactive radicals. Sensitizers with a barbiturate group at the meso-position preferred to bleach directly, while sensitizers carrying a cyclopentene moiety unexpectedly initiated the photosensitized mechanism.

Introduction

Oxime ester derivatives (R–CR'=N–OR'') were developed as photoinitiators to generate initiating radicals for radical photopolymerization.^[1] Excitation typically results in cleavage of the N–OR bond, resulting in the generation of two radicals, that is, R–CR'=N• and •OR''. Both are electrophilic radicals, facilitating addition onto (meth)acrylic monomers for the initiation of radical polymerization. Very early it became clear that substantial research must be pursued to improve the performance, that is, to match the absorption with available radiation sources and to improve thermal stability.^[2] Consequently, efforts proceeded to improve the match of absorption by introduction of appropriate substitution patterns, resulting in a bathochromic shift of the

absorption. The second point, that is, thermal stability, can still needs to be addressed. As a result, more research activities resulted in the commercialized oxime esters **OXE-01** and **OXE-02** (see Figure 1).^[3–6] Photophysical investigations and time-resolved spectroscopy helped to direct the development of such materials.^[7,8]

Recently, oxime esters comprising a coumarin structure, exhibiting a significant red bathochromic shift of absorption, enabled their use in combination with industrial UV-Blue LED devices.^[9] This finding has received attention since new regulations require the use of such light sources in new green and energy saving technologies.^[10] Thus, the improvements in thermal stability and bathochromic shifts of the absorption make them reliable photoinitiators for photopolymers in LED applications,^[11] which also have attracted attention in related two-photon excitations.^[12]

Besides the aforementioned improvements with respect to absorption and thermal stability, these derivatives also possess a significantly better compatibility with many environments. In particular, their use as coinitiators^[13,14] in digital imaging applications^[15–18] as alternatives to iodonium salts^[19] has many benefits. Iodonium salts and their tetraphenyl borates exhibit cytotoxicity,^[20] however such issues are not known for **OXE-01** and **OXE-02**. Iodonium salts also exhibit a certain thermal instability in combination with NIR sensitizers.^[21] In addition, they also exchange the anion with the NIR sensitizer in the case that these might be different, resulting in undesired crystallization of the NIR sensitizer in the light-sensitive layer. Thus, it is recommended that the same anion shall be used for both the cyanine and the iodonium cation together.^[19] This aspect might explain why these derivatives can be found in printing applications,^[13,14]

[*] Y. Pang, Q. Wang, D. Oprych, Prof. Dr. B. Strehmel
Department of Chemistry, Institute for Coatings and Surface
Chemistry, Niederrhein University of Applied Sciences
Adlerstr. 1, 47798 Krefeld (Germany)
E-mail: bernd.strehmel@hsnr.de

Y. Pang, S. Fan, Prof. Dr. Y. Zou
College of Chemistry, Beijing Normal University
No. 19, Xijiekouwai St. Haidian District
Beijing 100875 (P. R. China)
E-mail: zouyq@bnu.edu.cn

A. Feilen
EASYTEC GmbH
Pascalstr. 6, 52076 Aachen (Germany)

Dr. K. Reiner, Dr. D. Keil
FEW Chemicals GmbH
Technikumstraße 1, 06766 Bitterfeld-Wolfen (Germany)

Dr. Y. L. Slominsky
Institute of Organic Chemistry, National Academy of Sciences
Kiev 03094 (Ukraine)

Dr. S. Popov
Spectrum Info Ltd.
Murmanskaya 5, 02094 Kiev (Ukraine)

Supporting information and the ORCID identification number(s) for the author(s) of this article can be found under:
 <https://doi.org/10.1002/anie.202004413>.

© 2020 The Authors. Published by Wiley-VCH Verlag GmbH & Co. KGaA. This is an open access article under the terms of the Creative Commons Attribution Non-Commercial NoDerivs License, which permits use and distribution in any medium, provided the original work is properly cited, the use is non-commercial, and no modifications or adaptations are made.

applicable for development of on-press technologies as well.^[16,17] These technologies, based on excitation in the near-infrared at 830 nm, apply diode lasers for digital imaging.^[16–18] Fundamental knowledge is more or less in its infancy since most of the technological developments occurred in industry.

Recently, a review showed the potential of photopolymerization for many applications.^[22] Complementary studies about 3D and 4D printing extended the potential of photopolymerization.^[23] Furthermore, NIR excitation based on up-conversion nanoparticles enabled blue and UV light photoinitiators,^[24,25] while excitation at 980 nm resulted in a non-linear four-photon absorption process in the generation of UV light.^[26] An extensive review discussed the potential of free-radical and living radical polymerization.^[27] This potential is based mainly on UV and visible-light excitation, but NIR excitation did not address. Recently, an approach based on a photocatalytic system using Cu^{II} in combination with a cyanine comprising a barbiturate group also demonstrated applications in NIR-sensitized photopolymerization.^[28] Excitation based on NIR radiation has the advantage of i) deeper penetration into matter because of a significantly lower scattering coefficient,^[29] ii) embedding additives with UV absorption,^[10,30–32] and iii) the release of heat applicable for photothermal treatment of cancer cells.^[33] In particular, the introduction of new strongly emitting NIR-LED devices has brought about progress in this field.^[34] NIR light enabled photoinitiating systems comprising cyanines as the sensitizer and iodonium salts as the coinitiator work in free-radical polymerization systems.^[30] Photoinduced-electron transfer (PET) in most of these systems are based on an internal barrier, that is, low intensity NIR sources, and did not lead to initiation of photopolymerization.^[21] Interestingly, a combination of NIR photoinitiator systems with special additives also resulted in systems showing a certain tolerance to oxygen inhibition.^[35]

Cyanines with absorption in the NIR convert most of the absorbed light energy, as shown by the fluorescence quantum yield residing between 5 and 20% for systems requiring 800 nm excitation.^[15,21,28,36] This aspect has also received interest for industrial applications enabling thermally driven processes such as curing of blocked isocyanates^[10] or melting and crosslinking of powder coatings in just one step.^[37] This success has potential for replacing energy wasting furnace-driven processes by more ecologically LED techniques to design a system generating heat on demand.^[31,32] Although the development of LEDs has brought new impetus in this field,^[36] there still exists a demand for more alternative NIR-LED devices. This research introduces for the first time a new device emitting at 860 nm with an intensity of 1.5 W cm⁻². Nowadays, more research is focused on the design of alternative devices whose emission also covers the region between 900 and 1000 nm. This focus will help to substitute lasers emitting at 980 nm with more user-friendly LED devices.

The NIR-sensitized photoinitiated electron transfer (PET) mechanism has not been well explored based on fundamental research. The free energy of photoinduced electron transfer (ΔG_{et}) resides at either around zero eV or

is slightly negative for many cationic absorbers. The recently introduced model of internal activation of PET has brought new light in such systems.^[34,36] It resulted, in the case of iodonium salts, in bond cleavage of the cyanine chain, reduction of the iodonium salt, and therefore release of initiating radicals.^[36,38] Exposure of the absorber without any second component, except oxygen, also resulted in similar reaction products^[39–42] compared to systems explored with the NIR sensitizer and iodonium salt.^[38] Singlet oxygen might have a major function in the cleavage of the polymethine chain of the cyanine, while H₂O₂ and O₂⁻ were found to have minor reactivity with cyanines,^[42] although previous research showed that O₂⁻ played a major role in the photodegradation of cyanines.^[43] However, our previous experiments with a singlet oxygen microscope showed that almost no singlet oxygen was found, as already mentioned in Reference [38] (compare in this Ref. note 6). There were also synthesized many different structural motifs to explain the reactivity at distinct positions in the cyanine.^[44]

Shown herein for the first time is the NIR-sensitized decomposition of oxime esters, resulting in photoinitiation of radical polymerization. New high-power NIR-LEDs facilitate the decomposition of oxime esters. The question as to whether decomposition follows an entire photonic mechanism or thermal decomposition might play a certain function as well. Different structural motifs of the cyanines were chosen to determine PET leading either to chain breaking or changes of the polymethine structure with hypsochromically shifted absorption.^[13,14,28,36]

Results and Discussion

Figure 1 depicts the structural motifs of the oxime esters studied. While **OXE-01** and **OXE-02** represent state of the art in this field, **COXE-15**^[45] and **BTCF-OXE** depict new structures. **COXE-15** comprises a coumarin exhibiting hypsochromic-shifted absorption compared to alternative coumarins.^[9] This feature improves yellow safe light stability. Moreover, **BTCF-OXE** contains a new structural motif resulting in an improved thermal stability and comparable reactivity compared to **OXE-01** and **OXE-02**. Thermal treatment in tri(propylene glycol) diacrylate (**TPGDA**) resulted in an increase of the temperature for thermal initiation, T_i

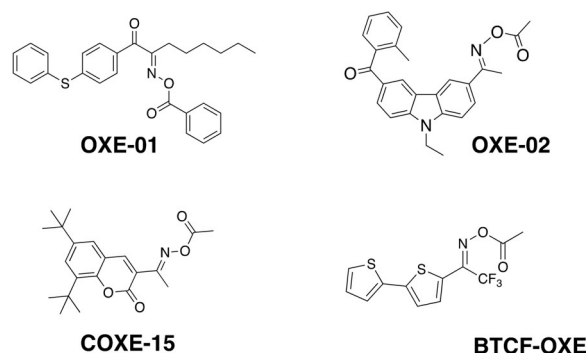


Figure 1. Structures of the oxime esters used.

Table 1: Results obtained for optical data (λ_{\max} : absorption maximum, ϵ : extinction coefficient), electrochemical data (E_{ox} : oxidation potential, E_{red} : reduction potential), initial temperature of intrinsic polymerization of **TPGDA** comprising NIR-sensitizer and oxime ester **OXE-01** T_i applying a gradient heating program up to 200 °C with a heating rate of 10 K min⁻¹,^[21] and final conversion x_{∞} obtained for photopolymerization of **TPGDA** followed by FTIR spectroscopy.

| Sens | λ_{\max} [nm] ^[b] | ϵ_{\max} [M ⁻¹ cm ⁻¹] | ϵ (805 nm) [M ⁻¹ cm ⁻¹] | ϵ (860 nm) [M ⁻¹ cm ⁻¹] | ϵ (395 nm) [M ⁻¹ cm ⁻¹] ^[c] | E_{ox} [V] ^[e] | E_{red} [V] ^[e] | T_i [°C] ^[d] | x_{∞} (805 nm) [%] ^[f] | x_{∞} (870 nm) [%] ^[f] | x_{∞} (395 nm) [%] ^[g] |
|--------------------------------------|---|--|--|--|---|---------------------------------------|--|------------------------------|---|---|---|
| TR ^[a] | 992 | 2.23×10^5 | – | – | – | 0.66 | –0.34 | 0 | 0 | 0 | – |
| 1bX₁ | 820 | 1.22×10^5 | 1.05×10^5 | 1.71×10^4 | – | 0.78 | –0.46 | 117 | – ^[h] | 60 ^[j] | – |
| 2bX₁ | 858 | 2.09×10^5 | 7.23×10^4 | 2.08×10^5 | – | 0.73 | –0.27 | 142 | 0 | 0 | – |
| 2bX₆ | ^[h] | ^[h] | – | – | – | ^[h] | ^[h] | – | 0 | 0 | – |
| 3baZ₁X₁ | 792 | 2.41×10^5 | 1.94×10^5 | 3.37×10^3 | – | 0.57 | –0.60 | 80 | 90 | 88 | – |
| 3baZ₁X₄ | 786 | 3.23×10^5 | 1.92×10^5 | 1.87×10^3 | – | 0.58 | –0.56 | 107 | 81 | 69 | – |
| 4aaZ₂ | 757 | 2.62×10^5 | 7.89×10^3 | < 0.1 | – | 0.41 | –0.86 | 92 | 78 | 68 | – |
| 4cβZ₃X₇ | 813 | 1.62×10^5 | 1.25×10^5 | 1.01×10^4 | – | 0.77 | –0.38 | 138 | 0 | 38 | – |
| 5dZ₄X₅ | 835 | 2.16×10^5 | 1.52×10^5 | 1.27×10^5 | – | 0.54 | –0.57 | 83 | – | 82 ^[j] | – |
| 6cZ₃X₃ | 844 | 2.39×10^5 | 9.92×10^4 | 1.32×10^5 | – | 0.56 | –0.57 | 80 | 0 | 90 | – |
| 6aZ₂ | 791 | 3.03×10^5 | 1.59×10^5 | 6.2×10^2 | – | 0.48 | –0.97 | 91 | 91 | 93 | – |
| OXE-01 | 326 | 2.95×10^4 | 0 | 0 | 6.43×10^2 | 1.72 | –1.36 | 65 ^[k] | – | – | 71 |
| OXE-02 | 337 | 2.30×10^4 | 0 | 0 | 2.48×10^2 | 1.51 | –1.26 | 68 ^[k] | – | – | 70 |
| COXE-15 | 300 | 1.65×10^4 | 0 | 0 | 4.00×10^2 | 1.59 | –1.30 | 78 ^[k] | – | – | 74 |
| BTCF-OXE | 356 | 2.28×10^4 | 0 | 0 | 3.76×10^2 | 1.70 | –1.26 | 173 ^[k] | – | – | 81 |

[a] From Ref. [21]. [b] In methanol. [c] In acetonitrile. [d] Onset temperature of the polymerization of **TPGDA**. [e] Final conversion of photopolymerization of **TPGDA** in the RT-FTIR measurement with 805 nm NIR-LED irradiation. [f] Final conversion of photopolymerization of **TPGDA** in the RT-FTIR measurement with 870 nm NIR-LED irradiation. [g] Final conversion of photopolymerization of **TPGDA** for the Photo-DSC measurement with 395 nm UV-LED irradiation. [h] Not determined because of structural similarity with **2bX₁**. [i] Conversion of photopolymerization of **TPGDA** after 10 min with 860 nm NIR-LED irradiation. [j] Not determined because of structural similarity with **3baZ₁X₁**. [k] Onset temperature of the polymerization of **TPGDA** without NIR sensitizer.

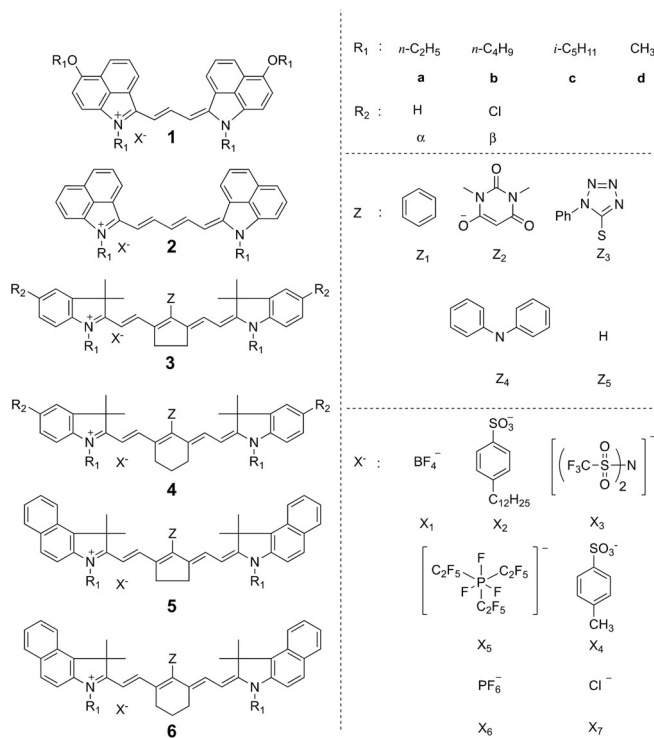
(Table 1). This temperature was below 70 °C for both **OXE-01** and **OXE-02**, while this quantity should only slightly increase for **COXE-15**. Surprisingly, T_i significantly increased in the case of the thiophene comprising the initiator **BTCF-OXE**, with an initial temperature for the start of thermal polymerization for **TPGDA** being close to that for the neat monomer without any other additive.^[21] Thus, one obtains the following stability of the oxime esters investigated:

BTCF-OXE \gg **COE-15** > **OXE-1** \approx **OXE-2**.

Further addition of a sensitizer to these mixtures resulted in a general improvement of thermal stability. T_i increased in general by about 50 K after adding the NIR sensitizers **1bX₁**, **2bX₁**, **2bX₆**, **3baZ₁X₄**, or **4cβZ₃X₇** while **3baZ₁X₁**, **4aaZ₂**, **5dZ₄X₅**, **6cZ₃X₃**, or **6aZ₂** resulted in a smaller increase (Table 1). Scheme 1 shows their structures. Nevertheless, the overall thermal stability increased after addition of the NIR sensitizer, ruling out the thermal instability of **OXE** as the only source for the reactivity observed upon NIR exposure. The cyanines **1** and **2**, which comprise no bridged structure, exhibited the best stability when combined with **OXE-01**.

Photoinitiated polymerization by LED exposure at 395 nm resulted in final double-bond conversion (x_{∞}) of about 70% in for **OXE-1**, **OXE-2**, and **COXE-15**. Thus, the structure of these three derivatives were not really affected by x_{∞} (compare the conversion–time profiles for the four derivatives of Figure 1 in Figure S11 in the Supporting Information). The derivative **BTCF-OXE** was the only representative showing a final conversion greater than 80%, although its initial reactivity was lower compared to the other three oxime ester compounds. Thus, the lower reactivity resulted in a higher overall final double-bond conversion because of higher selectivity.

The initiators **OXE-01**, **OXE-02**, and **COXE-15** were identified to initiate polymerization below 80 °C, bringing them to purposes requesting heat to generate radicals. Therefore, these initiators were tested in **TPGDA** comprising the cyanine **TR**, as shown in Figure 2, which nearly quanti-



Scheme 1. Structures of the cyanines **1–6** carrying different substituents, R_1 , R_2 , and Z .

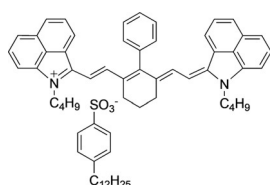


Figure 2. Structure of the sensitizer **TR** used for laser exposure at 980 nm.

tatively generates heat upon excitation at 980 nm. Such a radiation source facilitated initiation of thermally driven physical and chemical processes such as melting of powder coatings^[37] or the reaction of blocked isocyanates.^[10] There was no polymerization activity although the temperature increased to 170 °C as monitored by a thermal sensitive camera (for details see the Supporting Information). This increase of temperature did not result in thermal initiation of polymerization of **TPGDA** comprising **TR** and **OXE-01**. Thus, a mechanism requiring mainly heat to start **TPGDA** polymerization can be seen of minor importance. Previous investigations showed that **TR** contributes to the generation of heat.^[10,37]

This result shifted the strategy and the cyanines in Scheme 1 were selected for LED excitation at 805 nm, 860 nm, and 870 nm (new prototype). These devices exhibited intensities greater than 1 W cm⁻². Some of these cyanines were already found to work as sensitizers to generate initiating radicals for photopolymerization using an iodonium salt as the coinitiator in combination with a strongly emitting LED device.^[36] The oxime ester would function as the coinitiator.

According to the redox potentials shown in Table 1, the oxime esters may react according to a photoinitiated electron transfer (PET) based on a sensitized oxidation mechanism. A calculation of the reaction enthalpy of PET,^[46] ΔG_{et} , yields an overall endothermic scenario requiring thermal energy for the reaction (ΔG_{et} in eV: **6aZ₂** = 0.17; **3baZ₄X₁** = 0.27; **5dZ₄X₅** = 0.4). Furthermore, NIR-photopolymers comprising a cyanine and an iodonium salt possess an inner activation barrier (ΔG_{in}^{\ddagger}), which can exceed ΔG_{et} by several dozen kJ mol⁻¹,^[36] that is, $\Delta G_{in}^{\ddagger} > \Delta G_{et}$. These energetic conditions give such systems a certain inner threshold. The reaction only occurred in combination with a strong radiation source generating initiating radicals for photopolymerization, thus explaining their use for imaging purposes with a laser excitation at 830 nm.^[13,14,16] In this contribution, the LED devices emitting at either 805 nm, 860 nm, or 870 nm result in efficient generation of excited density whose deactivation and therefore also internal release of heat helps to overcome ΔG_{in}^{\ddagger} . To make it clear again, these systems work only in combination with strong emission sources. The use of such high-intensity LED-devices directs the system toward photopolymerization while low-intensity LEDs do not facilitate photopolymerization.

In this study, the sensitizer structures **1–6** generate initiating radicals to photopolymerize **TPGDA** by using strong irradiation sources. They comprise unbridged (**1,2**) and bridged (**3–6**) methine chains. The five-membered rings

in the centers of **3** and **5** keep the conjugated system in the plain while the structure at the center of **4** and **6** distorts the planarity, thus improving the solubility in certain environments.^[38] The compounds **1–6** comprise, depending on substitution pattern, different alkyl groups (R_1). Substitution at the *meso*-position also varies with change of the *Z* group. Furthermore, cyanine carries an anion X^- if it possesses a positive charge. Data compiled in Table 1 exhibit a larger bathochromic shift of absorption for NIR sensitizers comprising a benzo[*c,d*]indolium structure (**2**), in comparison with those having the same number of π electrons in the methine chain as for the benzo[*e*]indolium derivatives **3**.^[28] This aspect might have an impact on the color of the photoproducts. Oxidation of long methine chains often results in colored photoproducts.^[38,40–42] NIR-sensitizers with shorter chains should therefore exhibit less colorization upon exposure and in the presence of a coinitiator.

Embedding of the sensitizer **6aZ₂** in **TPGDA** together with the oxime esters shown in Figure 1 showed polymerization activity for **OXE-01**, **OXE-2**, and **COXE-15** upon using a strong emitting device at 805 nm, whereas **BTCF-OXE** showed no activity. The temperature increased to over 100 °C (Figure 3). Since the thermal equilibrium is attained between the surroundings and the substrate, the sample temperature remains between 100 and 110 °C (Figure 3). The change to a LED device with emission at 860 nm resulted in a slight change in pattern. At this wavelength, the absorber possesses a lower absorption. Therefore, the excitation light can penetrate deeper into the sample, resulting in reaction with the oxime ester and therefore also loss of absorption, explaining the temperature decrease in the case of **6aZ₂**. A photoreaction connected with bleaching results in the consumption of available sensitizer molecules, generating heat by internal conversion. The higher the concentration of the excited absorber molecules in the respective excitation volume, the higher the temperature generated. Exposure experiments followed by UV-VIS spectroscopy indicated a decrease of absorption. The lower the absorption of the NIR sensitizer, the lower the temperature generated (see Figure S19).

Figure 4 shows conversion–time profiles obtained for different NIR-sensitizers (**Sens**) in combination with the oxime esters of Figure 1. **OXE-01** showed the best performance in combination with **6aZ₂** (Figure 4a) while **OXE-2**, **COXE-15** and **BTCF-OXE** showed lower reactivity. PET may explain the observed reactivity although the enthalpy (ΔG_{et}) of PET is positive. This behavior is possible under some circumstances.^[43,46,47] The fact that **OXE-01** showed the best reactivity was surprising since the remaining oxime esters **OXE-2**, **COXE-15**, and **BTCF-OXE** exhibited similar reduction potentials but different thermal stability in **TPGDA**. Thus, heat generated by the NIR-sensitizer can also facilitate endothermic events because it contributes to a general increase of entropy. This additional energy released also helps the system to react so that **Sens** + **OXE** resulted in formation of **Sens⁺** and radicals. This reaction changes the number of molecules in the reaction and therefore the entropy of the system increases. The system investigated also possesses an internal activation energy differing for each type

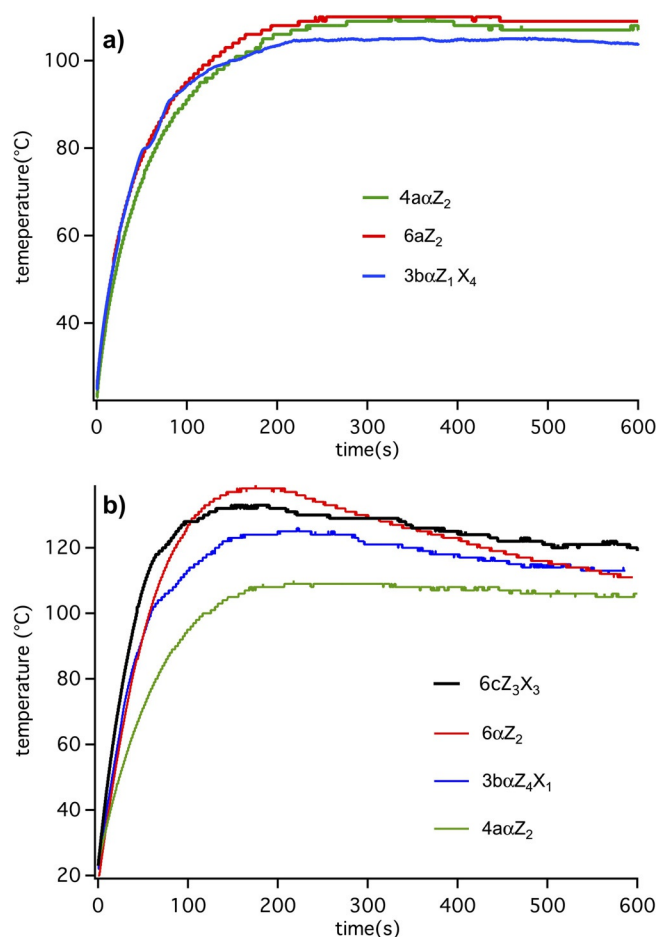


Figure 3. The temperature ($T/^\circ\text{C}$) generated by sensitizers (0.05 wt%) in the samples (thickness: 160 μm) comprising the monomer **TPGDA** and the oxime ester **OXE-01** (2Wt%). a) The samples were irradiated with the LED device from Phoseon at 805 nm having an intensity of 1.2 Wcm^{-2} . b) The samples were irradiated with the LED device from Easytech at 860 nm exhibiting an intensity of 1.5 Wcm^{-2} .

of sensitizer and **OXE**, explaining the different reactivities. The reaction between the sensitizer and the oxime ester also follows a bimolecular reaction as shown by the concentration variation of **OXE-1** in Figure 4b. In addition, the structure of the sensitizer also results in a different reactivity (Figure 4c). There was also no clear correlation between electrochemical data and reactivity with the oxime ester where **6aZ₂** showed the best reactivity and **4aαZ₂** showed the lowest efficiency. In this example, benzo[e]indolium derivatives exhibited higher reactivity compared to other indolium derivatives.

These findings led to the model of NIR-sensitized decomposition of oxime esters shown in Scheme 2. It is based on a mechanism where the combination of heat and chemical reactivity between the sensitizer **Sens** and the oxime ester **OXE** results in successful bleaching of **Sens** and initiating radicals as shown for the polymerization example in Figure 4. A mechanism based on thermal decomposition may be of minor importance because this cannot explain the bleaching of **Sens** observed. The heat generated may lead to decomposition as shown in part (a), but the optical density should remain constant. Laser exposure with a system generating

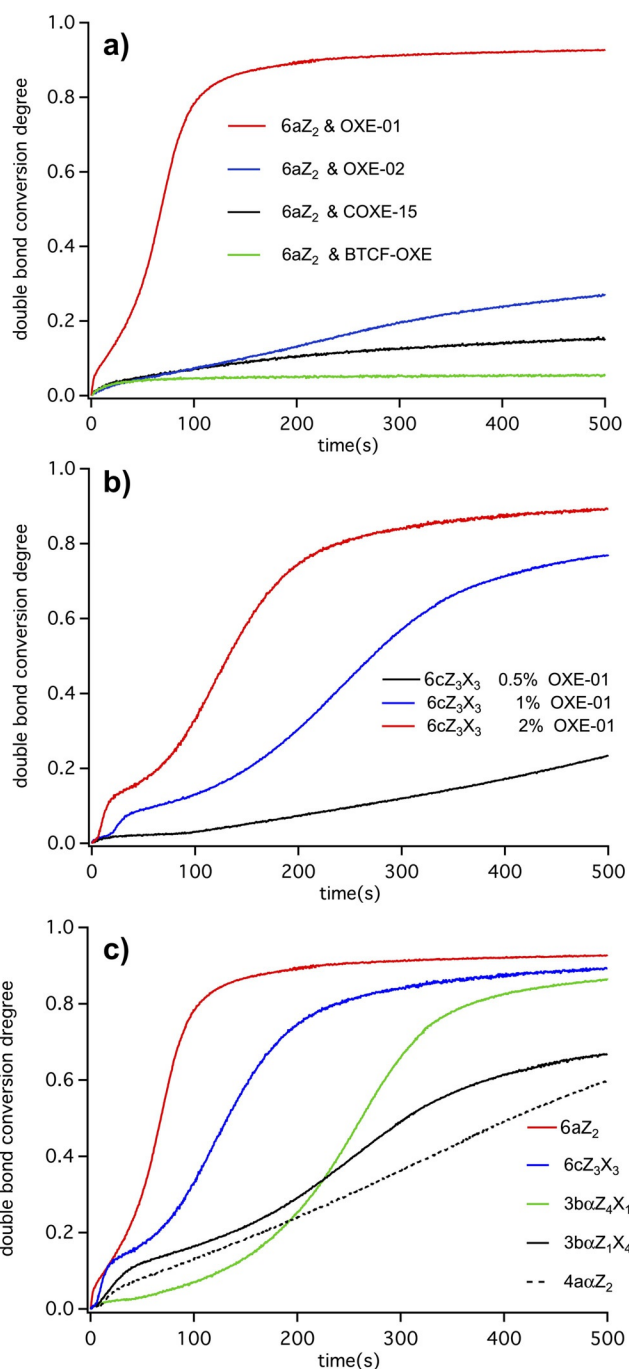
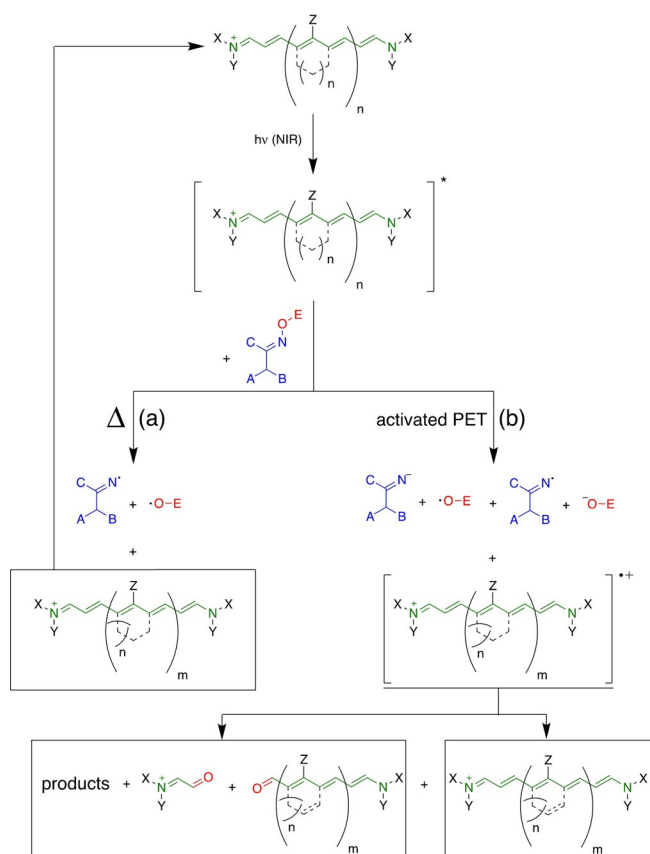


Figure 4. a) Radical photopolymerization of **TPGDA** with the sensitizer **6aZ₂** (0.05 wt%) and different oxime esters (2 wt%). b) Radical photopolymerization of **TPGDA** with the sensitizer **6cZ₃X₃** (0.05 wt%) and **OXE-01**, at different **OXE-01** concentrations (d). c) Radical photopolymerization of **TPGDA** with different sensitizers (0.05 wt%) and **OXE-01** (2 wt%). As excitation source served a NIR LED source emitting at 870 nm with an intensity of 1.2 Wcm^{-2} . Data were taken with a Bruker Vertex 70 in ATR-mode in real time (see the Supporting Information for more details).

mainly heat showed inefficient reaction based on route (a). More reasonable appears a mechanism where PET occurs over an activation barrier and the fact that heat additionally generated by thermal deactivation of **Sens** additionally results



Scheme 2. Proposal of possible reactions contributing to formation of radicals by NIR-sensitized activated photoinduced electron transfer.

in an increase of entropy. Exposure of **Sens** and **OXE** connects with the chemical reactivity resulting in formation of the respective reaction of the sensitizer as well. They were identified by reference materials^[13,14] synthesized and by LC-MS measurements.^[36,38] This can be cleavage of the polymethine chain resulting in the products bearing as terminal carbonyl group. These photoproducts exhibit yellow/brownish color as approved by the increased absorption between 400–600 nm^[38] (Figure 5 a). Exposure of sensitizers comprising a five-membered ring at the center of the cyanine resulted in photoproducts exhibiting a 100 nm hypsochromic-shifted absorption although they carry an additional bond. Figures 5 b and c depict the respective structures of the cyanine cations. Thus, the color changes to blue as previously confirmed for the sensitizer comprising the diphenyl amino group using an iodonium salt as the coinitiator.^[36] It turns out that a general a cyanine structure comprising either **3** or **5** favors formation of reaction products carrying an additional bond (see also the Supporting Information).

Figure 6 shows the kinetics of **3baZ₄X₁** and **3baZ₁X₄**. Because there was no total absorption, data obtained followed first-order kinetics. The sensitizer comprising the phenyl ring at the *meso*-position (**3baZ₄X₁**) exhibited a higher reactivity in the matrix, laurylmethacrylate (**LMA**), while the diphenylamino compound **3baZ₁X₄** showed lower reactivity upon exposure. This reactivity can differ by a change in

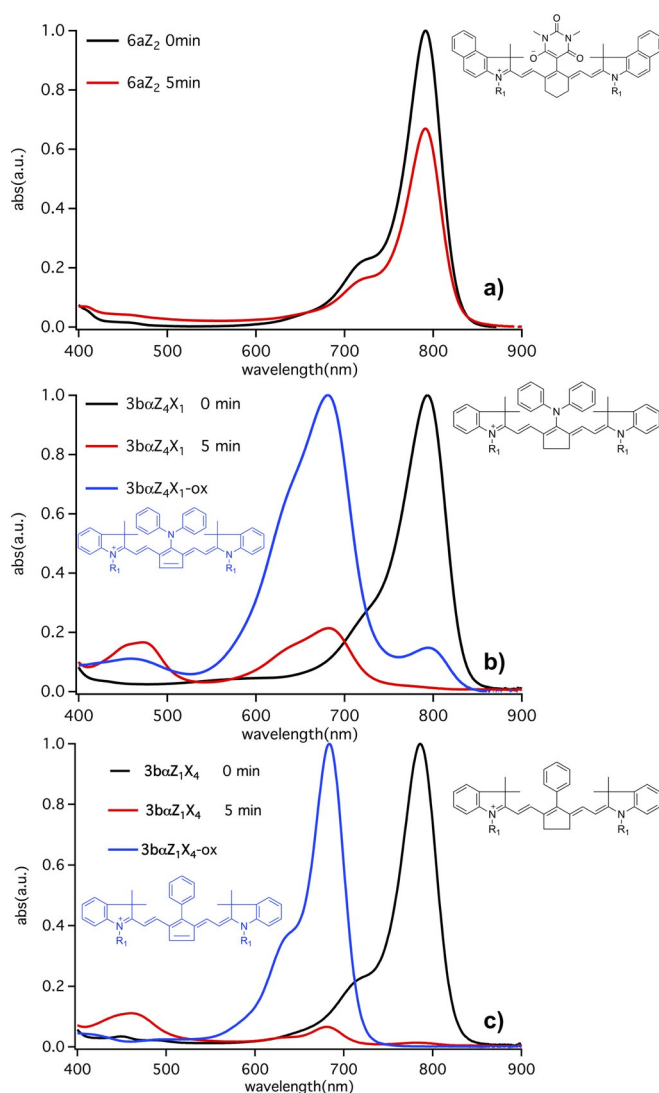


Figure 5. Change of UV/Vis-NIR spectra of **6aZ₂** (a), **3baZ₄X₁** (a), and **3baZ₁X₄** (a) upon exposure to NIR light at 805 nm applying an intensity of 1.2 Wcm⁻² and with **OXE-01** as coinitiator in **PEGMA**. The resulting polymer from **PEGMA** after LED exposure was dissolved in methanol and the measurement was done using a 1 cm × 1 cm cuvette. Figures 5 b and c depict the absorption of the respective oxidized product (blue). Exposure was pursued under nitrogen. For a sake of simplicity, only the cyanine structure was included.

the solvent, and also when oxygen is available during exposure (see the Supporting Information for more details).

Quantum-chemical calculations can explain the distinct electron distributions for **3daZ₁X₄** and its reaction product **3daZ₁X₄-ox** (Figure 7). This structure shows differences in the HOMO, where the oxidized product has a structure in the middle that is comparable with that of aromatic structures, an unsaturated moiety as with a cyanine (Figure 7). Conjugated aromatics typically depict an absorption located at shorter wavelength compared to cyanines.^[48] Calculations also confirmed the trend found in the experiments that reaction products exhibit lower absorption wavelength and absorption coefficient.

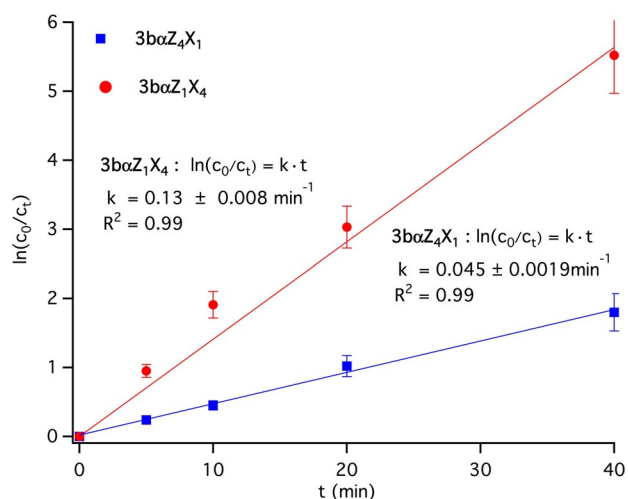


Figure 6. The kinetics of $3baZ_4X_1$ (blue) and $3baZ_1X_4$ (red). Samples comprising sensitizers ($3.5 \times 10^{-6} \text{ mol L}^{-1}$), **OXE-01** ($2.0 \times 10^{-5} \text{ mol L}^{-1}$), and **LMA** were irradiated with the 805 nm NIR LED device (1.2 W cm^{-2}) at different exposure times (for details see the Supporting Information).

Conclusion

The results obtained showed NIR-sensitized decomposition based on PET occurred. Heat released by nonradiative decomposition of the NIR-sensitizer plays a major function in this system as it results in an increase of entropy, promoting the occurrence of reactions under endothermic conditions and helping such a system to work although it possesses an internal activation barrier. These are two different points—thermodynamics and kinetics—explaining together the overall observed reactivity. This finding might affect the development of future technologies since their use requests strong emissive radiation sources in connection with systems having a certain daylight stability. This aspect makes easier handling possible under certain conditions in practice.

The blue color formed exhibits a further interesting feature. Thus, the methine chain remains in the oxidation process with no formation of reaction products exhibiting nucleophilic properties. This feature brings these materials also to systems facilitating cationic photopolymerization. Furthermore, the color formed might depict a further feature for systems requiring read-only in the exposed areas, which is the case in fully automatized CtP systems operating in on-press procedures in modern printing shops.

Future work might focus on the development of systems exhibiting a better compatibility with the environment. Introduction of the FAP-anion did not bring the expected effort. Potential exists to vary the alkyl substituent at the indolium ring since earlier investigations with similar materials showed promising results.

Acknowledgements

BS and YP acknowledge the Project D-NL-HIT carried out in the framework of the INTERREG-Program Deutschland-

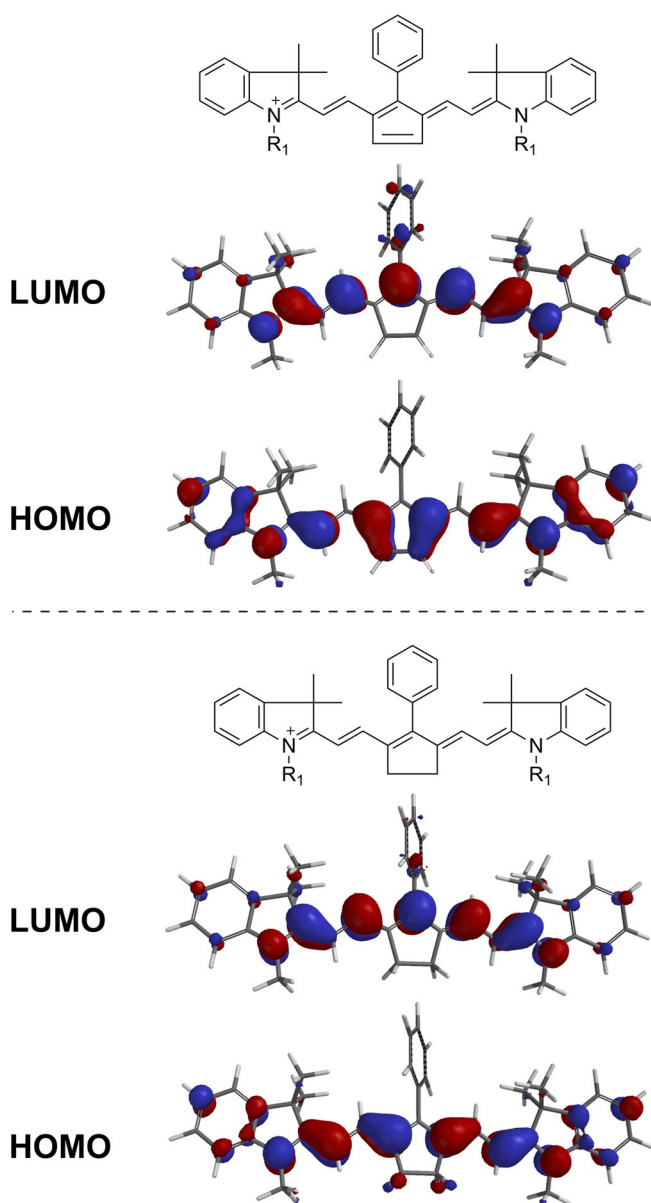


Figure 7. Electron density in the HOMO and LUMO of $3daZ_1X_4$ -ox obtained after a DFT calculation based on the B3LYP//6-31G* method implemented in Spartan 16 to optimize the ground state.

Nederland, which is co-financed by the European Union, the Mwide NRW, the Ministerie van Economische Zaken en Klimaat, and the provinces of Limburg, Gelderland, Noord-Brabant und Overijssel. BS additionally thanks the county of Nord Rhine-Westphalia for funding of the project REFU-BELAS (grant 005-1703-0006). We additionally thank the BMWi for funding the Project Innovative Nano-Coatings to support research at the Niederrhein University of Applied Sciences (ZF4288703WZ7) and FEW Chemicals GmbH (ZF4288702WZ7). We also thank Phoseon for providing the high-intensity 805 nm NIR-LED device. We also acknowledge Hubei Gurun Technology Co., Ltd for providing the oxime ester **GR-COXE-15**.

Conflict of interest

The authors declare no conflict of interest.

Keywords: aromatics · electron transfer · photochemistry · polymers · radicals

- [1] S. Il Hong, T. Kurosaki, M. Okawara, *J. Polym. Sci. Polym. Chem. Ed.* **1974**, *12*, 2553–2566.
- [2] K. H. Chae, *Macromol. Rapid Commun.* **1998**, *19*, 1–4.
- [3] K. Dietliker, R. Hüsler, J. L. Birbaum, S. Ilg, S. Villeneuve, K. Studer, T. Jung, J. Benkhoff, H. Kura, A. Matsumoto, H. Oka, *Prog. Org. Coat.* **2007**, *58*, 146–157.
- [4] K. Dietliker, T. Jung, J. Benkhoff, H. Kura, A. Matsumoto, H. Oka, D. Hristova, G. Gescheidt, G. Rist, *Macromol. Symp.* **2004**, *217*, 77–98.
- [5] J. Xu, G. Ma, K. Wang, J. Gu, S. Jiang, J. Nie, *J. Appl. Polym. Sci.* **2012**, *123*, 725–731.
- [6] X. Ma, R. Gu, L. Yu, W. Han, J. Li, X. Li, T. Wang, *Polym. Chem.* **2017**, *8*, 6134–6142.
- [7] D. E. Fast, A. Lauer, J. P. Menzel, A.-M. Kelterer, G. Gescheidt, C. Barner-Kowollik, *Macromolecules* **2017**, *50*, 1815–1823.
- [8] M. Griesser, A. Rosspeintner, C. Dworak, M. Höfer, G. Grabner, R. Liska, G. Gescheidt, *Macromolecules* **2012**, *45*, 8648–8657.
- [9] Z. Li, X. Zou, G. Zhu, X. Liu, R. Liu, *ACS Appl. Mater. Interfaces* **2018**, *10*, 16113–16123.
- [10] C. Schmitz, B. Strehmel, *J. Coat. Technol. Res.* **2019**, *16*, 1527–1541.
- [11] J. P. Fouassier, J. Lalevée, *Photoinitiators for Polymer Synthesis*, Wiley-VCH, Weinheim, **2012**.
- [12] W. Qiu, P. Hu, J. Zhu, R. Liu, Z. Li, Z. Hu, Q. Chen, K. Dietliker, R. Liska, *ChemPhotoChem* **2019**, *3*, 1090–1094.
- [13] Y. Iwai, K. Kunita (Fujifilm Corporation), EP 1849836 A2, **2007**.
- [14] Y. Iwai, K. Kunita (FUJIFILM Corporation), US 20070212643 A1, **2007**.
- [15] T. Brömme, C. Schmitz, D. Oprych, A. Wenda, V. Strehmel, M. Grabolle, U. Resch-Genger, S. Ernst, K. Reiner, D. Keil, P. Lüs, H. Baumann, B. Strehmel, *Chem. Eng. Technol.* **2016**, *39*, 13–25.
- [16] H. Baumann, T. Hoffmann-Walbeck, W. Wenning, H.-J. Lehmann, C. D. Simpson, H. Mustroph, U. Stebani, T. Telsler, A. Weichmann, R. Studenroth, *Ullmann's Encyclopedia of Industrial Chemistry*, Wiley-VCH, Weinheim, **2015**, pp. 1–51.
- [17] H. Baumann, *Chem. Unserer Zeit* **2015**, *49*, 14–29.
- [18] B. Strehmel, S. Ernst, K. Reiner, D. Keil, H. Lindauer, H. Baumann, *Z. Phys. Chem.* **2014**, *228*, 129–153.
- [19] C. Simpson, H. Baumann, B. Strehmel (Eastman Kodak Company), WO 2009109579 A1, **2009**.
- [20] T. Brömme, D. Oprych, J. Horst, P. S. Pinto, B. Strehmel, *RSC Adv.* **2015**, *5*, 69915–69924.
- [21] C. Schmitz, A. Halbhuber, D. Keil, B. Strehmel, *Prog. Org. Coat.* **2016**, *100*, 32–46.
- [22] N. Corrigan, J. Yeow, P. Judzewitsch, J. Xu, C. Boyer, *Angew. Chem. Int. Ed.* **2019**, *58*, 5170–5189; *Angew. Chem.* **2019**, *131*, 5224–5243.
- [23] Z. Zhang, N. Corrigan, A. Bagheri, J. Jin, C. Boyer, *Angew. Chem. Int. Ed.* **2019**, *58*, 17954–17963; *Angew. Chem.* **2019**, *131*, 18122–18131.
- [24] Z. Chen, D. Oprych, C. Xie, C. Kutahya, S. Wu, B. Strehmel, *ChemPhotoChem* **2017**, *1*, 499–503.
- [25] Z. Wu, K. Jung, C. Boyer, *Angew. Chem. Int. Ed.* **2020**, *59*, 2013–2017; *Angew. Chem.* **2020**, *132*, 2029–2033.
- [26] D. Oprych, C. Schmitz, C. Ley, X. Allonas, E. Ermilov, R. Erdmann, B. Strehmel, *ChemPhotoChem* **2019**, *3*, 1119–1126.
- [27] S. Dadashi-Silab, S. Doran, Y. Yagci, *Chem. Rev.* **2016**, *116*, 10212–10275.
- [28] B. Strehmel, C. Schmitz, C. Kutahya, Y. Pang, A. Drewitz, H. Mustroph, *Beilstein J. Org. Chem.* **2020**, *16*, 415–444.
- [29] M. Uo, E. Kudo, A. Okada, K. Soga, Y. Jogo, *J. Photopolym. Sci. Technol.* **2009**, *22*, 551–554.
- [30] C. Schmitz, D. Oprych, C. Kutahya, B. Strehmel in *Photopolymerisation Initiating Systems* (Eds.: J. Lalevée, J.-P. Fouassier), Royal Society of Chemistry, London, **2018**, pp. 431–478.
- [31] C. Schmitz, B. Strehmel, *Eur. Coat. J.* **2018**, *124*, 40–44.
- [32] C. Schmitz, B. Strehmel, *Farbe Lack* **2018**, *124*, 40–44.
- [33] Q. Xu, Y. Shen, Y. Zhang, X. Shao, *Bioorg. Med. Chem. Lett.* **2019**, *29*, 2398–2404.
- [34] B. Strehmel, C. Schmitz, K. Cremanns, J. Göttert, *Chem. Eur. J.* **2019**, *25*, 12855–12864.
- [35] A. H. Bonardi, F. Dumur, T. M. Grant, G. Noirbent, D. Gignes, B. H. Lessard, J. P. Fouassier, J. Lalevée, *Macromolecules* **2018**, *51*, 1314–1324.
- [36] C. Schmitz, Y. Pang, A. Gülz, M. Gläser, J. Horst, M. Jäger, B. Strehmel, *Angew. Chem. Int. Ed.* **2019**, *58*, 4400–4404; *Angew. Chem.* **2019**, *131*, 4445–4450.
- [37] C. Schmitz, B. Strehmel, *ChemPhotoChem* **2017**, *1*, 26–34.
- [38] T. Brömme, C. Schmitz, N. Moszner, P. Burtscher, N. Strehmel, B. Strehmel, *ChemistrySelect* **2016**, *1*, 524–532.
- [39] P. Chen, J. Li, Z. Qian, D. Zheng, T. Okasaki, M. Hayami, *Dyes Pigm.* **1998**, *37*, 213–222.
- [40] A. Samanta, M. Vendrell, R. Das, Y. T. Chang, *Chem. Commun.* **2010**, *46*, 7406–7408.
- [41] A. P. Gorka, R. R. Nani, J. Zhu, S. Mackem, M. J. Schnermann, *J. Am. Chem. Soc.* **2014**, *136*, 14153–14159.
- [42] R. R. Nani, J. A. Kelley, J. Ivanic, M. J. Schnermann, *Chem. Sci.* **2015**, *6*, 6556–6563.
- [43] C. Chen, B. Zhou, D. Lu, G. Xu, *J. Photochem. Photobiol. A* **1995**, *89*, 25–29.
- [44] L. Štacková, P. Štacko, P. Klán, *J. Am. Chem. Soc.* **2019**, *141*, 7155–7162.
- [45] Y. Pang, Y. Zou, S. Fan, Hubei Gurun Technology Co., Ltd., Peop. Rep. China. **2019**, p. 37.
- [46] G. J. Kavarnos, N. J. Turro, *Chem. Rev.* **1986**, *86*, 401–449.
- [47] G. J. Kavarnos in *Photoinduced Electron Transfer I* (Ed.: J. Mattay), Springer Berlin Heidelberg, Berlin, **1990**, pp. 21–58.
- [48] “Cyanine dyes”: H. Mustroph, *Physical Sciences Reviews* **2020**, <https://doi.org/10.1515/psr-2019-0145>.

Manuscript received: March 25, 2020

Revised manuscript received: April 21, 2020

Accepted manuscript online: April 29, 2020

Version of record online: May 11, 2020